

Precise QCD predictions on top quark pair production mediated by massive color octet vector boson at hadron colliders

Hua Xing Zhu,¹ Chong Sheng Li,^{1,2,*} Ding Yu Shao,¹ Jian Wang,¹ and C.-P. Yuan^{2,3,†}

¹*Department of Physics and State Key Laboratory of Nuclear Physics and Technology, Peking University, Beijing 100871, China*

²*Center for High Energy Physics, Peking University, Beijing 100871, China*

³*Department of Physics and Astronomy, Michigan State University, East Lansing, MI 48824, USA*

We present a theoretical framework for systematically calculating the next-to-leading order (NLO) QCD correction to the production of top quark pairs at hadron colliders, in a class of models with massive color octet vector bosons. We find that NLO corrections can decrease new physics cross section by about 50%, and top quark forward-backward asymmetry by 1–2%. The uncertainty in predicting the invariant mass distribution is reduced at NLO, and the shape of resonance is strongly modified by NLO corrections when taking the renormalization and factorization scales as the scale of top quark mass.

In many extensions of the Standard Model (SM), the massive Color Octet Vector Bosons (COVB) are necessarily engaged at the TeV scale. For example, in the top-color [1], warped (RS) or universal extra dimensions [2, 3], technicolor [4] and chiral color models [5]. In all these cases, the COVBs could have large impact on top quarks production, which are being copiously produced at the CERN Large Hadron Collider (LHC). With a large sample of $t\bar{t}$ data, CDF collaboration at the Tevatron has recently reported an observation of a large Forward-Backward asymmetry (A_{FB}) in $t\bar{t}$ production, $A_{\text{FB}}^{\text{tot}} = 0.158 \pm 0.075$, to be compared with the SM prediction 0.058 ± 0.009 . The disagreement is more significant in the region of large $t\bar{t}$ invariant mass, where CDF reported $A_{\text{FB}}(m_{t\bar{t}} > 450 \text{ GeV}) = 0.475 \pm 0.114$, and the SM gives 0.088 ± 0.013 [6]. This leads to more than 3.4σ deviation from the SM prediction [7], which resulted in extensive studies on this observable in various models beyond the SM. Among these, models with massive COVB are in particular attractive, c.f., Ref. [8] and references therein. A representative is the RS model [9]. However, those studies were all carried out at the leading order (LO) accuracy, and it's not clear whether the next-to-leading order (NLO) QCD corrections would change the conclusion.

The existence of such massive COVB will induce a resonant peak in the $t\bar{t}$ invariant mass distribution [10–13]. There have been substantial efforts in searching for narrow width resonant in $t\bar{t}$ production at the Tevatron and LHC. The recent analysis by CDF using 4.8 fb^{-1} integrated luminosity sees no evidence of resonant production of $t\bar{t}$ pairs in the lepton+jets channel, and a model with leptophobic Z' is excluded for $m_{Z'} < 900 \text{ GeV}$ [14]. Similar searches, but in semileptonic channel, for Z' with a narrow width have also been performed by the CMS and ATLAS collaborations at the LHC [15–18].

It is well known that QCD effects play an important role in $t\bar{t}$ production. The NLO QCD corrections to the SM $t\bar{t}$ production have been known for a long time [19–21]. It was found that the NLO corrections significantly

enhance the $t\bar{t}$ total cross sections and lead to large A_{FB} , although is still smaller than the current data. In the case of massive COVB, the QCD gauge interaction is uniquely determined by its color content, resembling a SM gluon. Therefore, it's reasonable to expect that QCD will also have significant effects on the processes mediated by the massive COVB, at least at an energy scale comparable to the mass of COVB. This has motivated the model dependent calculation of COVB production by gluon fusion [22] and the model independent (using dimension-six operators) calculation of $t\bar{t}$ production mediated by COVB [23]. However, a complete NLO analysis of the QCD effects to models with massive COVB in the resonant $t\bar{t}$ region is still absent.¹ In this letter, we present a model independent complete NLO QCD corrections to top quark pair production mediated by a general massive COVB, and show a detailed numerical analysis of top quark pair production, including invariant mass distribution and A_{FB} at the NLO level. We also show that the NLO corrections significantly stabilize the renormalization and factorization scale dependence, as compared to the LO results.

Below, we briefly outline our approach to systematically calculate the NLO QCD effects to processes with COVB production. We consider a model independent massive COVB originated from a broken $SU(3)$ gauge group. The effective Lagrangian in the unitary gauge can be written as

$$\mathcal{L}_G = -\frac{1}{2} \text{Tr} F_{\mu\nu} F^{\mu\nu} + M_G^2 \text{Tr} G_\mu G^\mu, \quad (1)$$

where $a = 1, \dots, 8$ is the broken $SU(3)$ “color” index, and $\mu = 0, \dots, 3$ is a Lorentz index. $F_{\mu\nu} = F_{\mu\nu}^a T^a$ is the field strength tensor, where T^a is the conventional Gell-mann matrix with the normalization $\text{Tr}[T^a T^b] = \frac{1}{2} \delta^{ab}$. The

¹ While this work was completed, Ref. [34] appeared, which calculates the singly production of color octet vector boson in the narrow width approximation.

mass of the COVB is denoted by M_G . The QCD color interaction between COVB and SM gluon can be easily implemented by changing the ordinary derivative into covariant derivative:

$$\partial_\mu G_\nu^a \rightarrow \partial_\mu G_\nu^a + g_1 f^{abc} A_\mu^b G_\nu^c, \quad (2)$$

where g_1 is the coupling constant of QCD. The Lagrangian in Eq. (1), after the replacement in Eq. (2), is already invariant under the conventional $SU(3)_c$ transformation. If desired, NLO QCD calculation can be done with the Feynman rule derived from the above Lagrangian, where unitary gauge is chosen for the broken $SU(3)$ gauge symmetry. However, it is well known that loop calculation in unitary gauge is inconvenient, because of the bad ultra-violet (UV) behavior of the propagator in unitary gauge. Instead, we choose to carry out the calculation in the conventional 't Hooft-Feynman gauge for the broken gauge group. For this purpose, we need to separate the longitudinal component (the would-be Goldstone boson) of the COVB from Eq. (1). This is done by modifying the mass term in Eq. (1) as follows,

$$G_\mu(x) \rightarrow U(x)^\dagger \left(\frac{i}{g_2} \partial_\mu + G_\mu(x) \right) U(x), \quad (3)$$

where we have introduced the π field (the would-be Goldstone field) via $U(x) = e^{i\pi^a(x)T^a/f}$, and the symmetry breaking scale $f = M_G/g_2$, with g_2 being the coupling constant of the broken $SU(3)$ gauge symmetry. It's easy to check that the mass term is now invariant under the gauge transformation:

$$G_\mu(x) \rightarrow V(x) \left(G_\mu(x) + \frac{i}{g_2} \partial_\mu \right) V(x)^\dagger, \quad (4)$$

$$U(x) \rightarrow V(x)U(x), \quad (5)$$

where $V(x)$ is a finite gauge transformation $V(x) = \exp(i\alpha_2^a(x)T^a)$. Similar to the unitary gauge, the interaction between G_μ , π and QCD gluon is obtained by changing the ordinary derivative to covariant derivative, as in Eq. (2). Expanding the mass term of the COVB in Eq. (1), we find that there is kinetic mixing between the COVB and the would-be Goldstone boson: $M_G \pi^a(x) \partial_\mu G_\mu^a(x)$. This mixing can be canceled by introducing the gauge fixing term:

$$F_2 = -\frac{1}{2}(\partial^\mu G_\mu^a(x) + M_G \pi^a(x))^2, \quad (6)$$

which is similar to the gauge fixing term for the SM QCD Lagrangian in 't Hooft-Feynman gauge. The ghost Lagrangian is given by

$$\mathcal{L}_g = \bar{u}^i(x) \frac{\delta F_i}{\delta \theta_j(x)} u^j(x), \quad (7)$$

where $i = 1$ for the SM QCD ghost, and $i = 2$ for the broken $SU(3)$ ghost. $\theta_i(x)$ are the infinitesimal gauge

transformation parameters for the corresponding gauge group. All the Feynman rules determined by gauge symmetry can then be derived. We have checked that this set of Feynman rules is in agreement with that derived in Ref. [24] for the case of Randall-Sundrum model [2].

Before continuing, we should define the precise meaning of the NLO QCD corrections in this paper. At the LO, there are three parts of contributions to the $t\bar{t}$ cross section in models with massive COVB: the squared SM amplitudes, the interference between the new physics (NP) amplitudes and the SM amplitudes, and the squared NP amplitudes. The NLO QCD corrections in this paper refer to the $\mathcal{O}(\alpha_s)$ corrections to these three parts separately. All the relevant Feynman rules can be derived from the effective Lagrangian given above. The results obtained in this way reflect the model independent corrections from QCD interaction. As a final comment, we note that our NLO QCD corrections are the non-Abelian analogy of the QED corrections to the W^\pm boson production process in hadron collision [25], and the neglected contributions in our calculation are similar to the genuine weak corrections there [25], which can be mostly absorbed into the redefinition of boson and fermion couplings at the LO.

Extending the approach shown in our paper [24], we calculate the one-loop renormalized helicity amplitudes, with the unstable particle treated in the complex mass scheme [26]. Loop integrals with complex arguments appear in the one-loop amplitudes are evaluated with ONELOOP [27]. Real emission matrix elements are generated by a modified version of MADGRAPH [28]. Soft and (or) collinear singularities of real corrections are dealt with by the dipole method [29], implemented in the MADDIPOLE package [30]. Throughout our calculation, the pole mass of top quark is chosen as $m_t = 173.1$ GeV, and $\alpha_s(M_Z) = 0.118$. LO cross sections are obtained using the CTEQ6L parton distribution functions (PDFs) [31] with one-loop running of α_s , while NLO cross sections are obtained using the CTEQ6M PDFs with two-loop running of α_s . In the numerical calculation below we present the results for a benchmark axial-gluon model [6]. As an example, the coupling between the massive COVB and quarks in these model are chosen as

$$v_q(m_t) = 0, \quad a_q(m_t) = 1.5, \quad (8)$$

$$v_t(m_t) = 0, \quad a_t(m_t) = -1.5, \quad (9)$$

where $g_1 v_{q(t)}$ and $g_1 a_{q(t)}$ are the vector and axial coupling of the light quark (top quark), defined at the scale m_t . The evolution of $v_{q,t}(\mu)$ under the change of scale is given by $v(\mu)_{q,t} = v(\mu_0)_{q,t} (\alpha_s(\mu)/\alpha_s(\mu_0))^{15/(2\beta_0)}$ [24], where $\beta_0 = 23/3$ is the LO QCD beta function for $N_c = 3$ and $n_f = 5$. The evolution equation of $a_{q,t}(\mu)$ has the same form as $v_{q,t}(\mu)$. Unless specified, the mass of the COVB is chosen as 1.5 TeV.

First we define the NP cross section, σ_{NP} , as the difference between $t\bar{t}$ cross section in a model with a new massive COVB, and the SM:

$$\sigma_{\text{NP}} = \sigma_{\text{SM+NP}} - \sigma_{\text{SM}}. \quad (10)$$

The SM cross sections, including both the $q\bar{q}$ - and gg -channel, are calculated with the program MCFM [32].

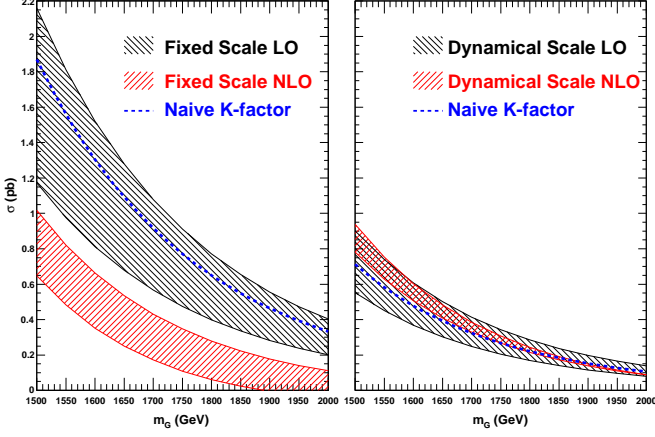


FIG. 1. σ_{NP} , defined in Eq. (10), as functions of M_G for two different benchmark schemes. The black (red) bands are the LO (NLO) uncertainties, estimated by varying the scales around their default values by a factor of two within each scheme. The blue dashed lines are the naive estimates of the NLO effects by simple rescaling of the LO results with the SM K-factor.

In Fig. 1, we plot the NP contribution to the cross section at the LHC with $\sqrt{s} = 7$ TeV, as a function of M_G . The bands reflect the scale uncertainties estimated by varying the renormalization and factorization scales around their default values by a factor of two. We present the results in two benchmark schemes, namely the fixed scale scheme, where the scales are fixed to be m_t , and the dynamical scale scheme, where the scales are set to be the invariant mass of the top quark pair $m_{t\bar{t}}$. We find that the NLO QCD effects are much larger (by about 50%) in the fixed scale scheme than the dynamical scheme for our choice of parameters, and the naive estimate of the NLO effects by simple rescaling of the LO results with the SM NLO K-factor is not appropriate. It is also clear that the inclusion of NLO QCD effects strongly reduces the theoretical uncertainty of the NLO cross section in either scheme, comparing with the LO ones, as expected.

Fig. 2 gives the LO and NLO invariant mass distribution of the top quark pair at the LHC with $\sqrt{s} = 7$ TeV, including contribution from the SM LO and NLO top quark pair production. It can be seen that in the fixed scale scheme, NLO QCD corrections significantly change the shape of the LO curve, leading to the reduction of

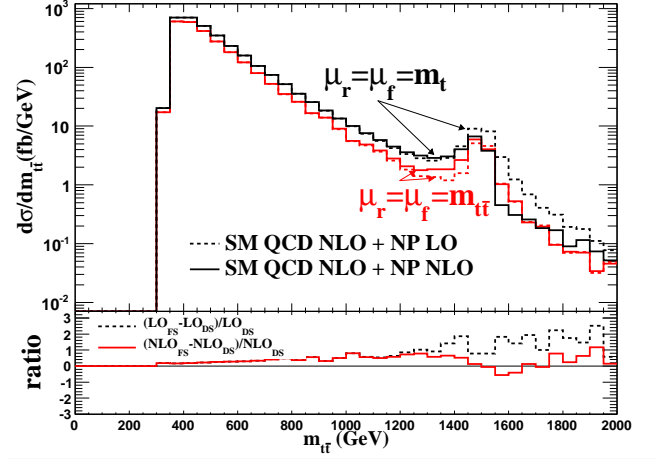


FIG. 2. LO (dashed lines) and NLO (solid lines) invariant mass distribution of the top quark pair at the LHC with $\sqrt{s} = 7$ TeV. Also shown are the differences between two different schemes at the LO and NLO.

the width of the resonance, which is important for accurate extraction of the mass and width of resonance from $t\bar{t}$ invariant mass distribution experimentally. The NLO width can be expressed analytically as

$$\frac{\Gamma_{\text{NLO}}(\mu)}{\Gamma_{\text{LO}}(\mu)} = \left[1 + \frac{\alpha_s(\mu)}{\pi} \left(\frac{167}{12} - \pi^2 - \frac{15}{4} \ln \frac{M_G^2}{\mu^2} \right) \right]. \quad (11)$$

From Eq. (11), it's obvious that the width of COVB is reduced at the NLO when $\mu = m_t$, and the large logarithmic contribution can be canceled by a dynamical scale choice $\mu = m_{t\bar{t}}$. This is confirmed in Fig. 2, where the NLO results for the dynamical scale scheme has relatively small corrections comparing with the LO one. The predictions in the two scheme at the NLO level are close to each other, while at the LO level they show large difference, as shown in the lower panel of Fig. 2. The difference between the two schemes reflects the uncertainty of the theoretical prediction. Hence, the NLO result leads to a smaller theoretical uncertainty in $m_{t\bar{t}}$ distribution, which could improve the accuracy of extracting the theory parameters of NP models from comparing to experimental data. We also note that similar conclusion holds in other cases, e.g., KK gluon in RS model.

Fig. 3 shows the LO and NLO contribution to the A_{FB} as a function of the mass of the COVB at the Tevatron with $\sqrt{s} = 1.96$ TeV in the center of mass frame of the $t\bar{t}$ pair. The results are given for both the total asymmetry and the asymmetry in the large invariant mass region, $m_{t\bar{t}} > 450$ GeV, respectively. As we know, the NLO QCD corrections in the SM enhance the A_{FB} comparing with the LO results [7], but the NP contributions at the NLO level only reduce the A_{FB} by 1 – 2%. Similar behaviors are also found for vector-like coupling (not shown).

in this paper). Therefore the LO predictions for A_{FB} are stable against the NLO QCD corrections. This increases the confidence on the massive COVB explanation of the Tevatron A_{FB} anomaly. If this anomaly can be further confirmed, it could be a first hint of new physics signal.

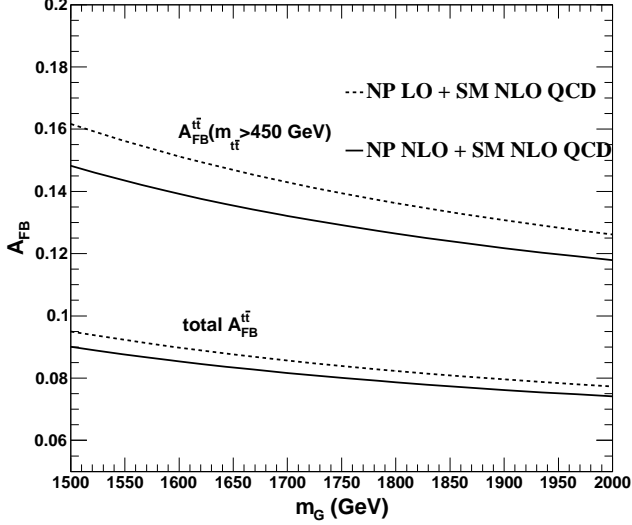


FIG. 3. NP contributions to the A_{FB} in the $t\bar{t}$ center of mass frame as a function of the mass of the COVB at the Tevatron with $\sqrt{s} = 1.96$ TeV. In the upper lines only the A_{FB} in the large invariant mass region, $m_{t\bar{t}} > 450$ GeV, are plotted, while in the bottom total A_{FB} are shown.

As a further application of our results, we plot in Fig. 4 the NP cross section, σ_{NP} , for a specific RS model considered in the Ref. [18]. Also plotted are the experimental exclusion limit extracted from the same paper. Our exact theoretical predictions are given for three different scale choices, $\mu = m_t$, $\mu = M_G$ and $\mu = m_{t\bar{t}}$, for both the LO and NLO. It can be seen that while the NLO QCD effects are moderate in the $\mu = m_{t\bar{t}}$ case, they are large in both the $\mu = m_t$ and $\mu = M_G$ cases. We also plot in Fig. 4 the LO results (the black solid line) with only the contributions from NP squared amplitudes, i.e., without the interference with the SM amplitudes. It's clear in Fig. 4 that considering the NP squared amplitudes contributions alone obviously underestimates the NP cross section, and including the interference contributions is necessary for reliable predictions. We note that while the mass limit for KK gluon is very different at the LO for the three kinds of scale choices, their differences are significantly reduced at the NLO. Hence, the NLO results can be used for precise extraction of mass limit for KK gluon.

In conclusion, we have presented a theoretical framework for systematically calculating the NLO QCD effects to various experimental observables predicted by mod-

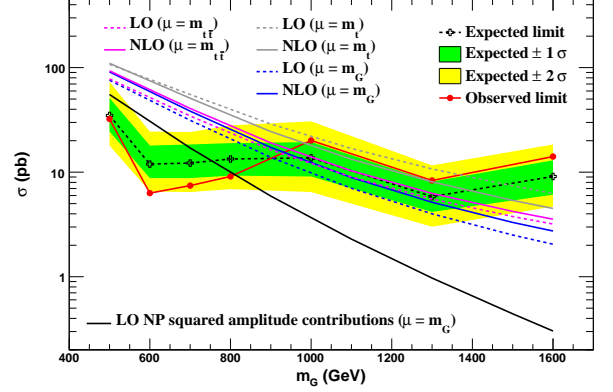


FIG. 4. LO and NLO predictions for σ_{NP} in a specific RS model [18]. The expected and observed limits on cross section are extracted from the Ref. [18].

els with massive COVB, in a model independent way. Specifically, we have showed the numerical results of the NLO QCD corrections to the total cross sections, invariant mass distribution and the A_{FB} of the top quark pairs produced by mediating a massive COVB. Our results show that, for our choice of parameters, the NLO corrections of the NP cross section are much larger in the fixed scale scheme than in the dynamical scale scheme, and the naive estimate of the NLO effects by simple rescaling of the LO results with the SM NLO K-factor is not appropriate. We have also showed that the NLO QCD corrections only reduce the A_{FB} by 1 – 2%, as compared to the LO prediction. This result leads to increased confidence on the massive COVB models explanations of the top quark A_{FB} observed at the Tevatron by CDF [6] and D0 collaborations [33]. Moreover, for the invariant mass distribution, we find that the NLO QCD corrections reduce the width of the resonant particle in the fixed scale scheme (with $\mu \sim m_t$), and therefore change the shape of the distribution, and the effects of the NLO QCD corrections can be suppressed in the dynamical scale scheme. The difference in the results using the fixed scale and dynamical scale schemes indicates the size of theoretical uncertainty in our predictions, and we have showed that the uncertainty is reduced by the inclusion of NLO QCD effects.

We would like to thank Liang Dai and Jun Gao for collaboration on early stage of this project, and Qing-Hong Cao, Michele Pettei, Bernd Stelzer, and Jing Shu for helpful discussion. This work was supported in part by the National Natural Science Foundation of China, under Grants No.11021092 and No.10975004. C.P.Y acknowledges the support of the U.S. National Science Foundation under Grant No. PHY-0855561.

* csli@pku.edu.cn

† yuan@pa.msu.edu

- [1] C. T. Hill, Phys. Lett. **B266**, 419 (1991).
- [2] L. Randall and R. Sundrum, Phys. Rev. Lett. **83**, 3370 (1999).
- [3] T. Appelquist, H.-C. Cheng, and B. A. Dobrescu, Phys. Rev. **D64**, 035002 (2001).
- [4] K. D. Lane and M. V. Ramana, Phys. Rev. **D44**, 2678 (1991).
- [5] J. C. Pati and A. Salam, Phys. Rev. Lett. **34**, 613 (1975).
- [6] T. Aaltonen et al. (CDF), Phys. Rev. **D83**, 112003 (2011).
- [7] O. Antunano, J. H. Kuhn, and G. Rodrigo, Phys. Rev. **D77**, 014003 (2008).
- [8] J. F. Kamenik, J. Shu, and J. Zupan (2011), 1107.5257.
- [9] A. Djouadi, G. Moreau, and F. Richard, Phys. Lett. **B701**, 458 (2011).
- [10] K. Agashe, A. Belyaev, T. Krupovnickas, G. Perez, and J. Virzi, Phys. Rev. **D77**, 015003 (2008).
- [11] B. Lillie, L. Randall, and L.-T. Wang, JHEP **09**, 074 (2007).
- [12] R. Frederix and F. Maltoni, JHEP **01**, 047 (2009).
- [13] U. Baur and L. H. Orr, Phys. Rev. **D77**, 114001 (2008).
- [14] T. Aaltonen et al. (The CDF) (2011).
- [15] **The CMS Collaboration**, CMS PAS TOP-10-007.
- [16] **The CMS Collaboration**, CMS PAS EXO-11-006.
- [17] **The CMS Collaboration**, CMS PAS EXO-11-055.
- [18] **The ATLAS collaboration**, ATLAS-CONF-2011-123.
- [19] P. Nason, S. Dawson, and R. Ellis, Nucl.Phys. **B303**, 607 (1988).
- [20] W. Beenakker, H. Kuijf, W. van Neerven, and J. Smith, Phys.Rev. **D40**, 54 (1989).
- [21] W. Beenakker, W. van Neerven, R. Meng, G. Schuler, and J. Smith, Nucl.Phys. **B351**, 507 (1991).
- [22] B. C. Allanach, F. Mahmoudi, J. P. Skittrall, and K. Sridhar, JHEP **03**, 014 (2010).
- [23] M. Bauer, F. Goertz, U. Haisch, T. Pfoh, and S. Westhoff, JHEP **1011**, 039 (2010).
- [24] H. X. Zhu et al., JHEP **09**, 043 (2011).
- [25] D. Wackeroth and W. Hollik, Phys.Rev. **D55**, 6788 (1997).
- [26] A. Denner and S. Dittmaier, Nucl. Phys. Proc. Suppl. **160**, 22 (2006).
- [27] A. van Hameren (2010), 1007.4716.
- [28] J. Alwall, M. Herquet, F. Maltoni, O. Mattelaer, and T. Stelzer, JHEP **1106**, 128 (2011).
- [29] S. Catani, S. Dittmaier, M. H. Seymour, and Z. Trocsanyi, Nucl. Phys. **B627**, 189 (2002).
- [30] R. Frederix, T. Gehrmann, and N. Greiner, JHEP **06**, 086 (2010).
- [31] P. M. Nadolsky et al., Phys. Rev. **D78**, 013004 (2008).
- [32] J. Campbell, K. Ellis, and C. Williams, *Mcfm - monte carlo for femtobarn processes*, <http://mcfm.fnal.gov>.
- [33] V. M. Abazov et al. (D0) (2011), 1107.4995.
- [34] R. Chivukula, A. Farzinnia, R. Foadi, and E. H. Simmons (2011), 1111.7261.